Copy 658

NASA TM X-29

TECHNICAL MEMORANDUM
X - 29

PREFLIGHT AND FLIGHT INVESTIGATION ON A DUCTED SOLID-PROPELLANT ROCKET CONFIGURATION AT MACH NUMBERS FROM 1.56 TO 2.14

By Walter L. Kouyoumjian and Donald C. Tolefson

Langley Research Center
Langley Field, Va.

UNCLASSIFIED

N71-73427
(ACCESSION NUMBER)
(PAGES)
(NASA CR OR TMX OR AD NUMBER)
(THRU)
None
(CODE)
(CATEGORY)
FACILITY FORM 602

NASA TM X-29 5/20/71

NATIONAL AERONAUTICS AND SPACE ADMINISTRATION
WASHINGTON
August 1959

Z

[redacted]

NATIONAL AERONAUTICS AND SPACE ADMINISTRATION

TECHNICAL MEMORANDUM X-29

PREFLIGHT AND FLIGHT INVESTIGATION ON A DUCTED SOLID-PROPELLANT ROCKET CONFIGURATION AT MACH NUMBERS FROM 1.56 TO 2.14*

By Walter L. Kouyoumjian and Donald C. Tolefson

SUMMARY

A preflight-jet and free-flight investigation was made at the NASA Wallops Station on a ducted rocket propulsive system which incorporated an annular conical-shock nose inlet to supply additional air to a solid-fuel sustainer rocket mounted in the inlet afterbody. In order to determine the performance characteristics of the system, preflight tests were made in the 27- by 27-inch preflight-jet of the NASA Wallops Station at a free-stream Mach number of 1.8, Reynolds numbers per foot from 4.57×10^6 to 9.9×10^6, and zero angles of attack and yaw. The maximum gross thrust for the preflight test was 1,175 pounds with a gross thrust coefficient of 0.864. The specific impulse based on propellant weight was 582 lb-sec/lb, whereas the specific impulse based on weight of air was 286 lb-sec/lb.

The flight investigation was made at flight Mach numbers from 1.56 to 2.14 and Reynolds numbers per foot from 9.95×10^6 to 10.92×10^6. The model flew in a near-zero-lift trajectory after separation from a booster and accelerated from a free-stream Mach number of 1.56 to approximately 2.14 before the model failed. The gross thrust coefficient varied from approximately 0.49 to 0.54 through the flight Mach number range. A value of instantaneous fuel specific impulse of 350 lb-sec/lb at a free-stream Mach number of 2.14 was determined by using calculated values of propellant flow rate and gross thrust coefficient.

INTRODUCTION

Preflight and free-flight tests were made at the NASA Wallops Station on a ducted rocket model. Inasmuch as it is inherently the

[redacted]

nature of solid-fuel rocket motors to burn fuel rich, the present model employs a supersonic inlet as a method of supplying additional air to the solid-fuel sustainer rocket mounted in the inlet afterbody. The models used in the investigation were supplied by the Thiokol Chemical Corporation, Huntsville, Alabama.

The model was tested at zero angle of attack in the preflight jet with a free-stream Mach number of 1.8 and Reynolds numbers per foot range from 4.57×10^6 to 9.9×10^6, with and without the sustainer rocket motor burning.

The flight test of the model was conducted at Mach numbers from 1.56 to 2.14 and at Reynolds numbers per foot from 9.95×10^6 to 10.92×10^6. The model flew in a near-zero-lift trajectory throughout the flight Mach number range.

This report presents a summary of the preflight-jet and free-flight data.

SYMBOLS

A	area, units as specified when used
a	acceleration, ft/sec^2
$C_{D,x}$	external-drag coefficient, $Drag/q_\infty S$
C_T	thrust coefficient, $T/q_\infty S$
F	thrust, lb
g	acceleration due to gravity, 32.2 ft/sec^2
M_∞	free-stream Mach number
p	static pressure, lb/sq in. abs
p_t	total pressure, lb/sq in. abs
$p_{t,x}$	total pressure in model combustion chamber, lb/sq in. abs
$p_{t,\infty}$	free-stream total pressure, lb/sq in. abs
p_∞	free-stream static pressure, lb/sq in. abs

q_∞	free-stream dynamic pressure, lb/sq in. abs, $\frac{1}{2}p_\infty M_\infty^2$
R	Reynolds number per foot
S	reference area, model frontal area 0.238 sq ft
T	temperature, deg Rankine
t	time, sec
w	weight of model, lb
w/w_∞	mass-flow ratio based on free-stream capture area
γ	flight-path angle, deg

MODELS

The model consisted of a conical-shock annular nose inlet with a solid-fuel sustainer rocket motor mounted in the inlet afterbody, with an Inconel sheet combustion chamber and a sonic nozzle at the exit station. The model was stabilized by using three 45° sweptback fins mounted on the combustion-chamber shell. The sustainer rocket motor served as a gas generator for the ram air supplied by the nose. The additional combustion (afterburning) occurred in the combustion chamber downstream of the inlet and sustainer-rocket-motor location. The final products of combustion were exhausted through a convergent nozzle with an exit exhaust Mach number of 1.00.

Sketches and photographs of the models and exploded views of the details of the components are presented in figures 1 to 5. Photographs of the model in the preflight jet before the ground jet phase of the investigation are presented as figures 6(a) and (b). The calculated internal-area distributions of the model from reference 1 are presented in figure 7.

PREFLIGHT INVESTIGATION

Description of Preflight Tests and Instrumentation

The ground tests of the ducted rocket configuration were made in the preflight jet of the NASA Wallops Station at a free-stream Mach number of 1.8 and included hot and cold runs (with and without the

sustainer rocket motor burning). Figures 6(a) and 6(b) show a three-quarter rear view and a side view, respectively, of the model in the preflight jet prior to a test. The model was mounted longitudinally at zero angles of attack and yaw so that the inlet entrance plane was slightly behind the jet exit plane and inside the "test diamond" of the jet when the jet was started. The instrumentation used was a force stand to which the model support stand was attached in a fashion that would indicate all the longitudinal loads acting on the model and the portion of the support stand immersed in the air stream. During the cold tests a pressure survey rake was mounted behind the model and located at the model nozzle exit plane, whereas for the hot test a single total-pressure tube was mounted in the model exit plane. It was assumed that the total pressure in the model exit plane was equal to the total pressure in the combustion chamber. The pressure data were taken by using pressure transducers and recorded by a multichannel recording oscillograph.

L 3 2 5

Preflight Test Results and Discussion

The measured data from the ground tests are presented in figures 8 to 15. Figure 8 presents the tunnel conditions of total pressure and q_∞ under which the ground tests were conducted. A graph of the combustion-chamber total pressure plotted against the total pressure of the jet is presented in figure 9. The average pressure ratio presented in this figure for $p_{t,jet}$ between 70 and 110 lb/sq in. abs. agrees well with a theoretical pressure ratio of 0.359 using conical-shock theory and one-dimensional flow considerations. Figure 10 presents the inlet mass-flow ratio as a function of jet total pressure. In the equation for mass-flow ratio

$$\frac{W}{W_\infty} = \frac{p_x M_x A_x \sqrt{T_x}}{p_\infty M_\infty A_{inlet} \sqrt{T_\infty}}$$

the subscript ∞ refers to free-stream conditions at inlet design Mach number whereas the subscript x refers to free-stream conditions at other Mach numbers. This equation for mass-flow ratio is based on choked flow at the model exit minimum section and refers to a free-stream stagnation temperature of 810° R. The dashed-line curve in figure 10 is the maximum mass-flow ratio possible for an inlet designed for Mach number 2.00 operating at a free-stream Mach number of 1.80. This value for maximum critical mass-flow ratio, for an inlet operating below design Mach number, is from reference 2. This ratio is for an external compression inlet operating at the maximum mass-flow ratios, whereas the present inlet has a small amount of internal compression

which may account for some of the apparent 4-percent mass-flow spillage for these tests.

Figure 11 presents the data from a total-pressure tube at the model exit plane for the hot tests. The curve shows a time lag of 2.25 seconds between ignition and when the total pressure in the combustion chamber peaks and reaches its operating level. Shadowgraphs of the sequence indicated that the inlet external flow field was not markedly affected by the changes in combustion-chamber pressure and operated near the critical mass-flow ratio as shown in figure 10. Figure 12 presents the results of the cold run and shows the force-stand readings which include the drag of the model mounting stand and the computed internal drag (ref. 2) from the results of the pressure survey rake at the model exit plane. The external drag curve in figure 12 is the difference of the force-stand reading and the computed internal drag. Figure 13 presents the force-stand reading during the hot run with the sustainer rocket burning. The difference between the external drag curve (also plotted in fig. 13) and the power-on force-stand readings is the model gross thrust. (See fig. 14.) The maximum gross thrust achieved during the preflight tests was 1,175 pounds with a maximum gross thrust coefficient of 0.864. The average gross thrust was found to be 724 pounds from figure 14, and the average thrust coefficient was 0.514 from figure 15. The gross thrust variation shown appears to be because of the internal rocket thrust characteristics; however, generally speaking, the results of the ground tests indicated that this method of propulsion was functional and feasible. An additional conclusion from figure 13 is that it substantiates the results from figure 12; the two curves are coincident during the ignition time lag between 4 and 5.25 seconds; also, the time lag and the subsequent variation in model thrust corresponds closely to the variation in exit total pressure presented in figure 11.

Figure 14 presents the gross thrust for the ground test plotted against time. From this figure the specific impulse based on total thrust and total propellant weight is 582 lb-sec/lb whereas the specific impulse based on the total air flow is 286 lb-sec/lb. Figure 15 presents the model gross thrust coefficient $C_{T,gross}$ plotted against time.

The accuracy of the data presented herein is within 2 percent of maximum values for all experimental and computed results.

FLIGHT INVESTIGATION

Description of Flight Test

A photograph of the model and booster on the launcher prior to firing is presented as figure 16. The model was launched at an angle

of 60° from a zero length rail launcher and was boosted by a JATO unit T55. The model flew in a near-zero-lift trajectory and was tracked from the ground by CW Doppler radar for velocity and NASA modified SCR-584 radar for trajectory. The sustainer rocket had a 2.2-second delay squib at which time the sustainer rocket ignited and the model accelerated away from the booster motor. The sustainer rocket motor burned for approximately 6 seconds at which time the SCR-584 radar tracking indicated the model had exploded, probably as a result of overheating of the combustion chamber. Ambient conditions were measured after the flight with a balloon-carried rawinsonde.

Flight Test Results

The flight test results are presented in figures 17 to 21; the accuracy of the results is within the order of 2 percent of the full-scale reading. The thrust coefficient was computed from

$$C_{T,net} = \frac{W}{gq_\infty S}(a + g \sin \gamma)$$

where a was obtained by differentiating the velocity time curve from the CW Doppler radar, and q and γ were obtained from the flight conditions along the trajectory.

Figure 17 presents the model flight trajectory with the broken section, after approximately 8 seconds, indicating the time of the model failure. Figure 18 presents the model Reynolds number per foot as a function of the Mach number. Figure 19 presents the curves of the model acceleration against time. It should be noted here that figure 19 indicates that the model began accelerating at about 2.6 seconds after take-off; hence, there was not the anticipated time lag of approximately 2.25 seconds which was noted in figure 11 for the ground tests. This difference may be due to the fact that the model exit area was choked by the presence of the booster rocket motor and therefore the model combustion-chamber pressure was higher than its equivalent during the ground test. Figure 20 presents the free-stream Mach number plotted against time. Figure 21 presents the curves of model external drag coefficient $C_{D,x}$ estimated by using references 2, 3, and 4, the model net thrust coefficient $C_{T,net}$ which was computed from flight data by multiplying the model acceleration (fig. 19) with model weight from reference 1, and the model gross thrust coefficient $C_{T,gross}$ which is the sum of the net thrust coefficient and external-drag coefficient. The average thrust coefficients from ground tests and as computed from

RESTRICTED

stoichiometric burning at a Mach number of 1.8 are shown in figure 15. For stoichiometric burning at a Mach number of 1.8, a gross propellant specific impulse of 755 lb-sec/lb was calculated by considering a combustion efficiency of 80 percent. The method of this calculation is from equation (1) of reference 1, and the following values obtained from reference 1 are used:

Specific gas constant at afterburner nozzle exit	51.6
Ratio of specific heats	1.3
Mach number at afterburner nozzle exit	1.00
Total temperature at afterburner nozzle exit, ^{o}R	3,937
Free-stream Mach number	1.8

The gross thrust was determined to be 1,232 pounds with a constant propellant weight flow of 1.63 lb/sec (ref. 1), and a value for $C_{T,stoichiometric}$ of 1.07 was calculated. The model instantaneous fuel specific impulse was calculated by using the gross thrust coefficient and fuel-flow data from reference 1. The results of instantaneous fuel specific impulse were 329 at a free-stream Mach number of 2.04 and 350 at a free-stream Mach number of 2.14.

CONCLUDING REMARKS

The results of the preflight tests indicate that the inlet external flow field was not affected markedly by high combustion-chamber pressures encountered at start of combustion due to rocket-motor ignition. The maximum gross thrust achieved during the preflight tests was 1,175 pounds with a maximum gross thrust coefficient of 0.864 and the average gross thrust developed was 724 pounds with an average gross thrust coefficient of 0.514. The specific impulse based on propellant weight was 582 lb-sec/lb, whereas the specific impulse based on weight of air was 286 lb-sec/lb.

After the model separated from the booster, the model accelerated from a Mach number of 1.56 to a Mach number of 2.14. Model failure may have been due to either a failure of the thin combustion-chamber wall, due to heat and pressure, or due to the rocket motor exploding. The gross thrust coefficient varied from approximately 0.49 to 0.54 through the flight Mach number range. A maximum calculated value of instantaneous fuel specific impulse of approximately 350 lb-sec/lb at a free-stream Mach number of 2.14 was determined from the gross thrust coefficient and calculated propellant flow rates.

Langley Research Center,
National Aeronautics and Space Administration,
Langley Field, Va., March 23, 1959.

[redacted]

REFERENCES

1. Blalock, Ralph: Flight Ducted Rocket No. 3 - Aerodynamic, Propulsion, and Performance Data. TM-26, Thiokol Chemical Corp., Redstone Div. (Huntsville, Ala.), 1957.

2. Sibulken, Merwin: Theoretical and Experimental Investigation of Additive Drag. NACA Rep. 1187, 1954. (Supersedes NACA RM E51B13.)

3. Fraenkel, L. E.: Curves for Estimating the Wave Drag of Some Bodies of Revolution, Based on Exact and Approximate Theories. C. P. No. 136, British A.R.C., 1953.

4. Van Driest, E. R.: Turbulent Boundary Layer in Compressible Fluids. Jour. Aero. Sci., vol. 18, no. 3, Mar. 1951, pp. 145-160, 216.

I
3
2
5

[redacted]

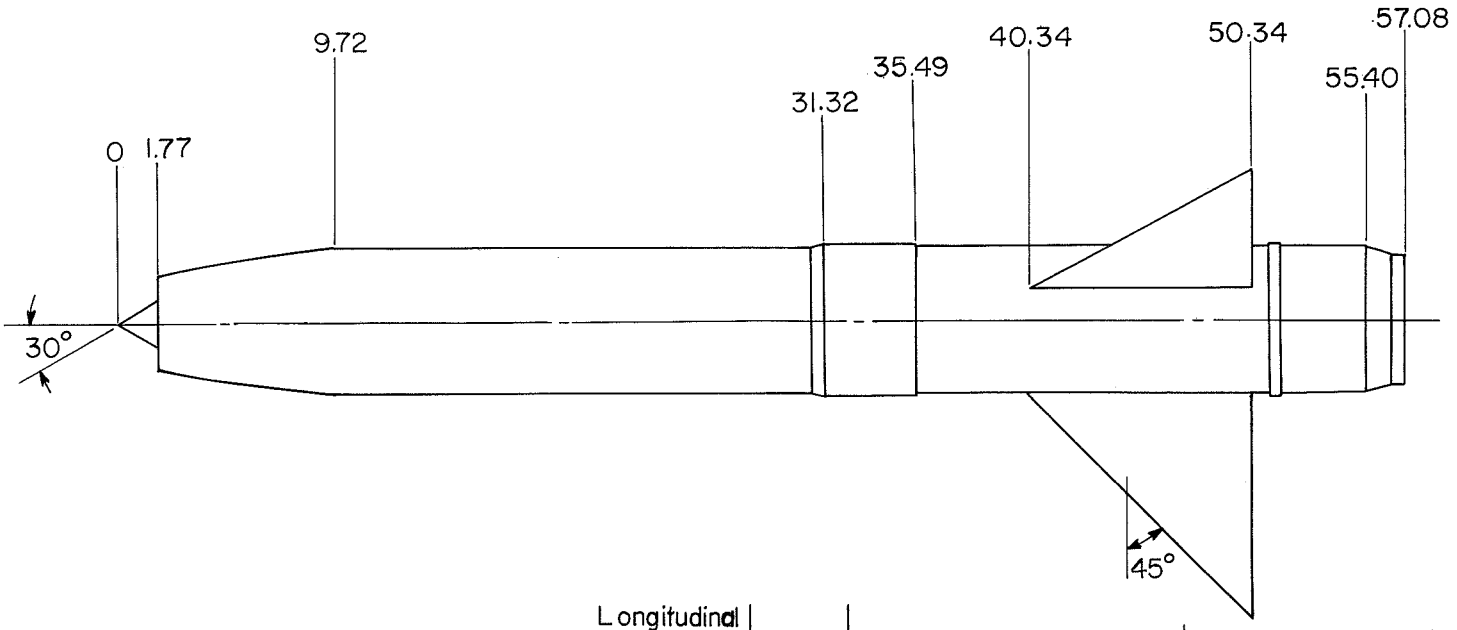

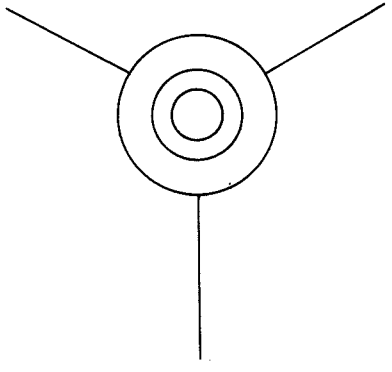

Longitudinal station	Radius
0	0
1.77	1.98
9.72	3.31
31.32	3.47
35.49	3.27
51.00	3.32
55.40	3.27
57.08	2.96
Nozzle exit	2.72

	Wt, lb	Length, in.	c.g. sta.
Model and booster(loaded)	112.8	98.81	53.8
Booster propellant	33.4		
Model (loaded)	55.2	57.08	30.5
Sustainer propellant	13.6		

Figure 1.- General sketches of model. All dimensions are in inches unless otherwise stated.

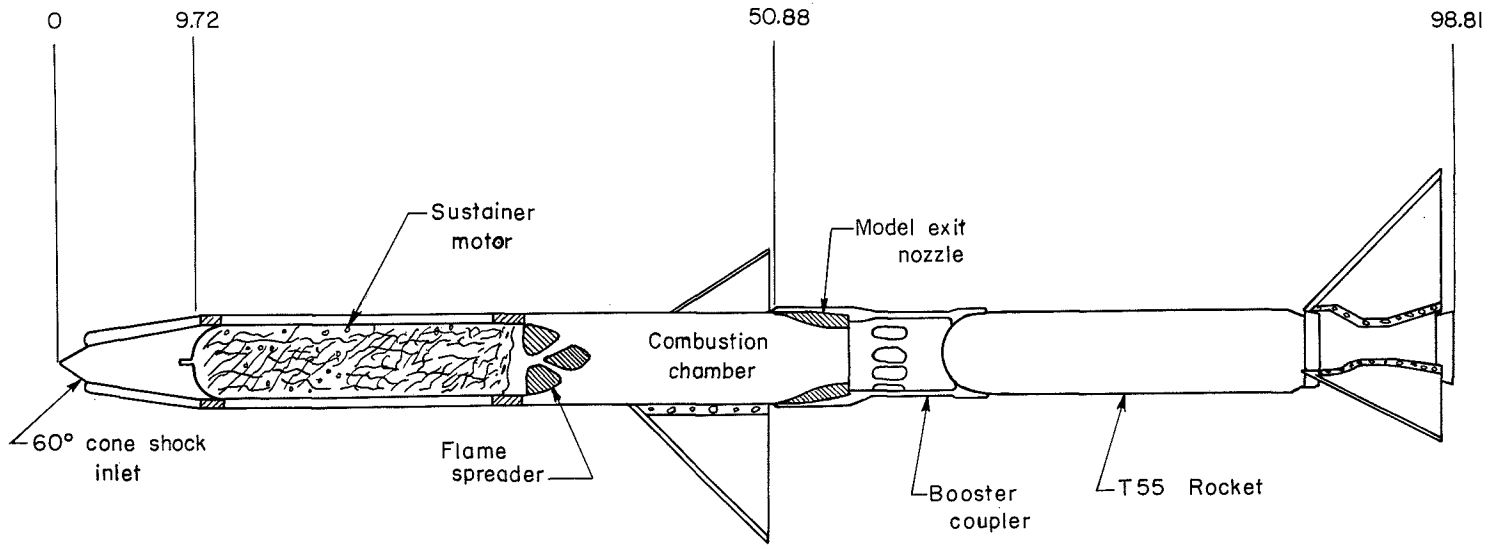

Figure 1.- Concluded.

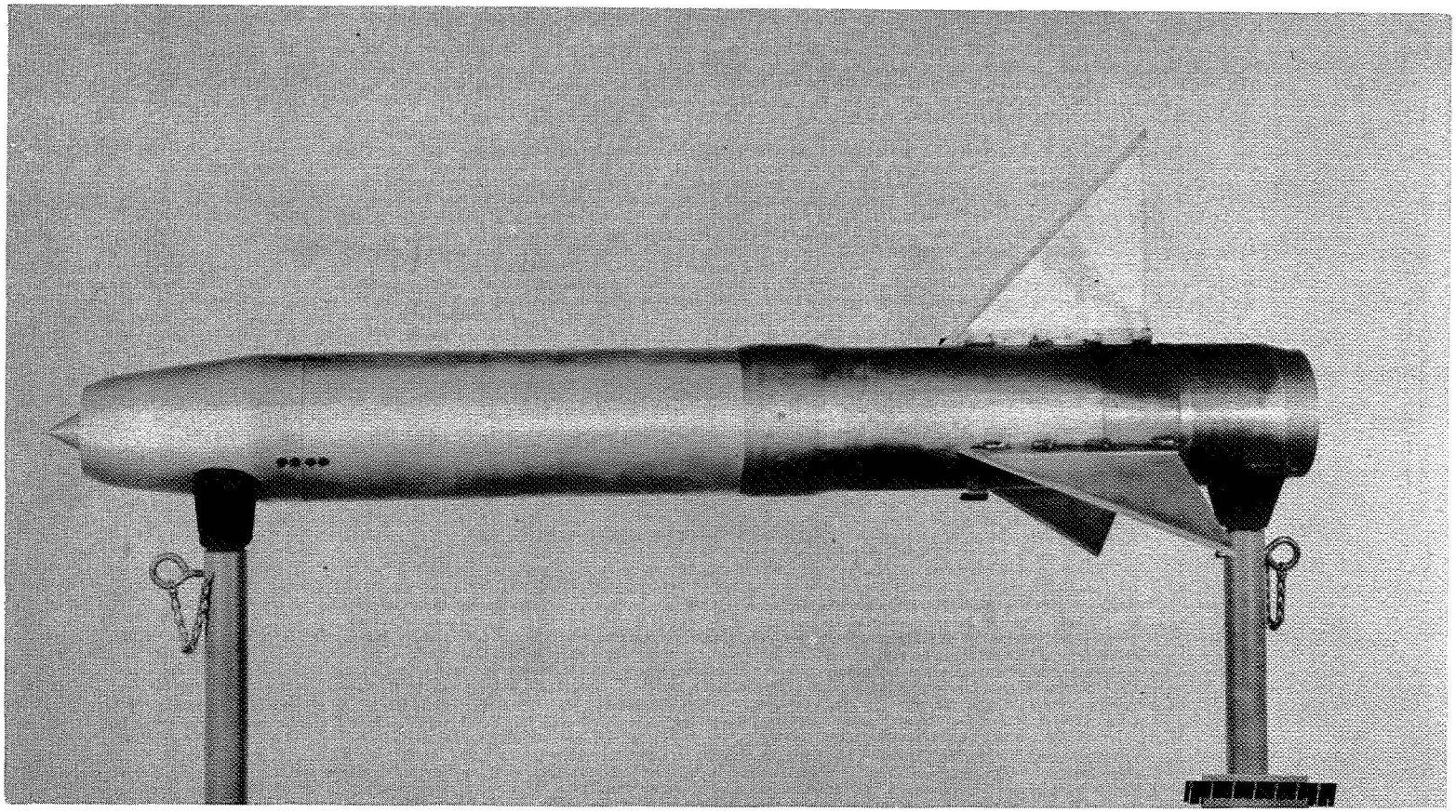

Figure 2.- Side view of ducted rocket model. L-57-4701

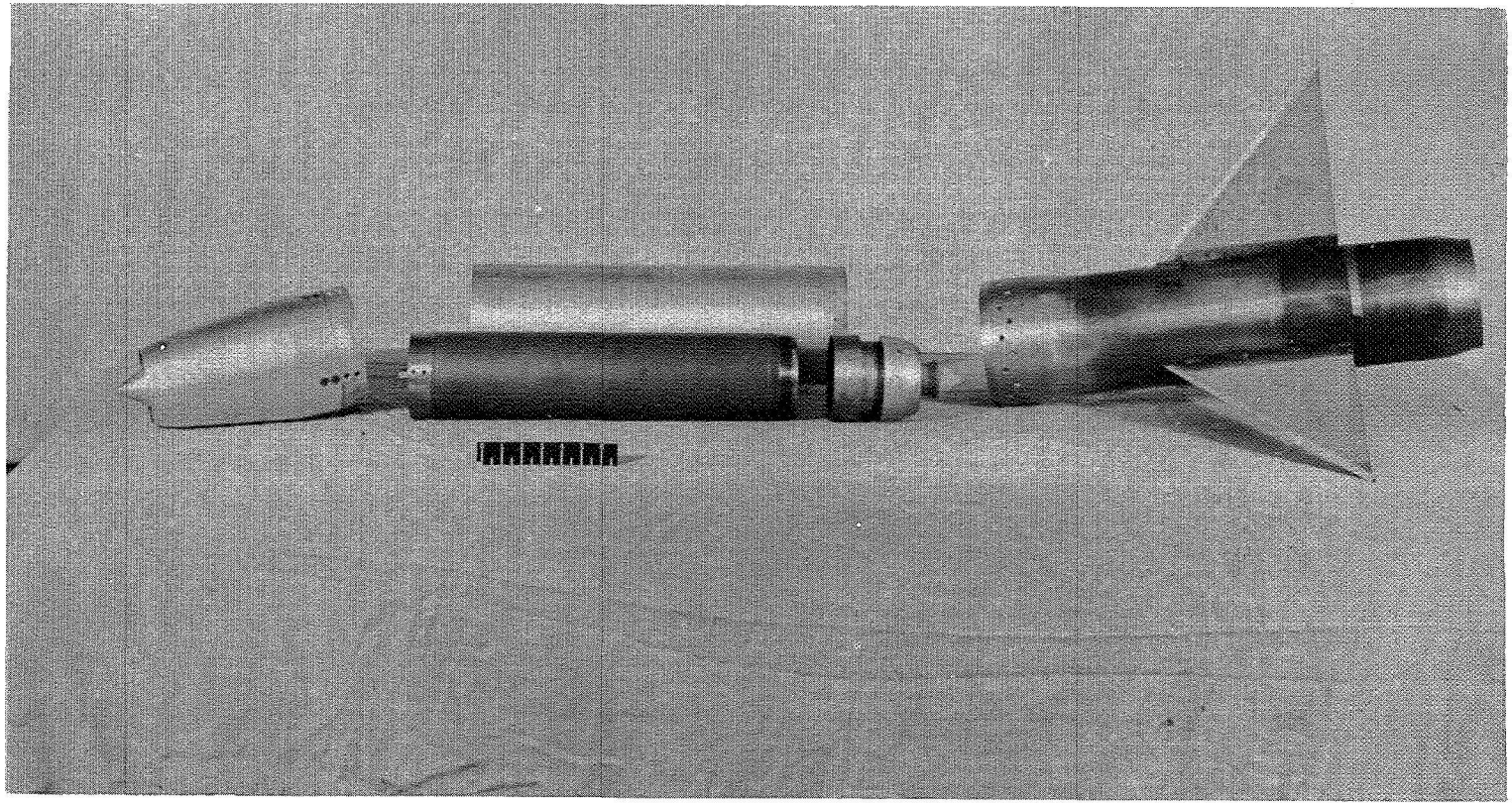

Figure 3.- Disassembled parts of ducted rocket model. L-57-4703.1

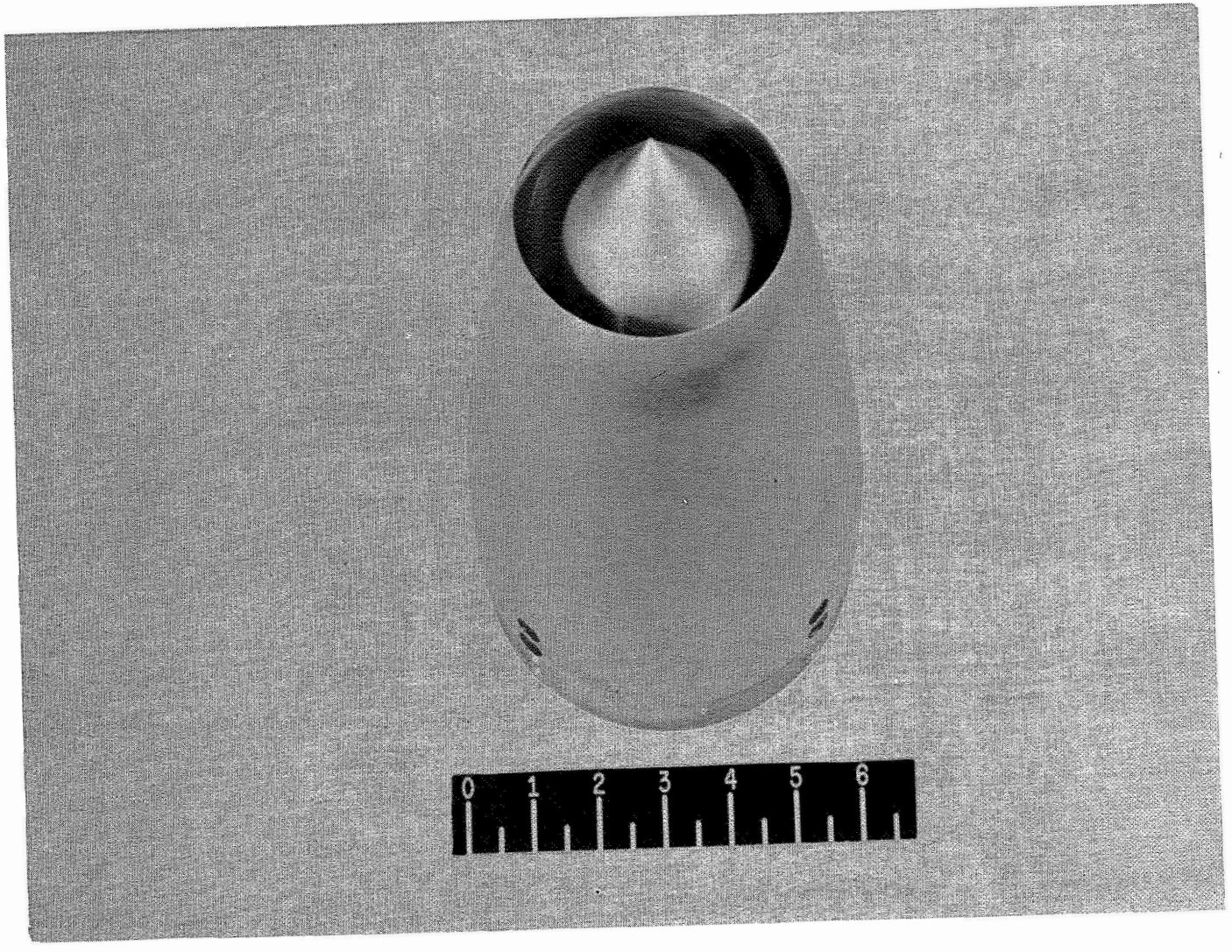

Figure 4.- Nose-inlet detail. L-57-4705.1

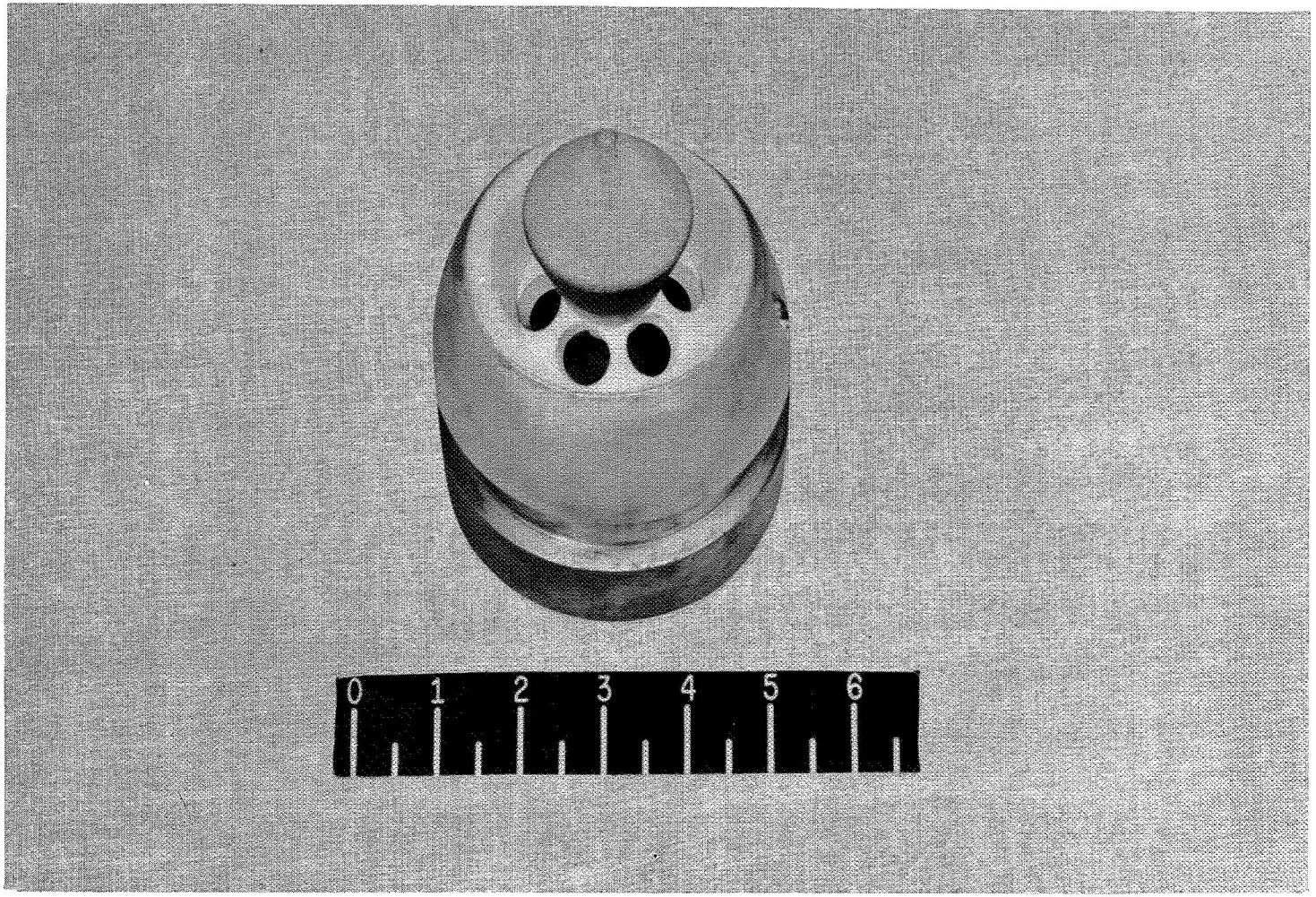

L-57-4704.1

Figure 5.- Detail of sustainer rocket-motor flame spreader showing dispersion holes.

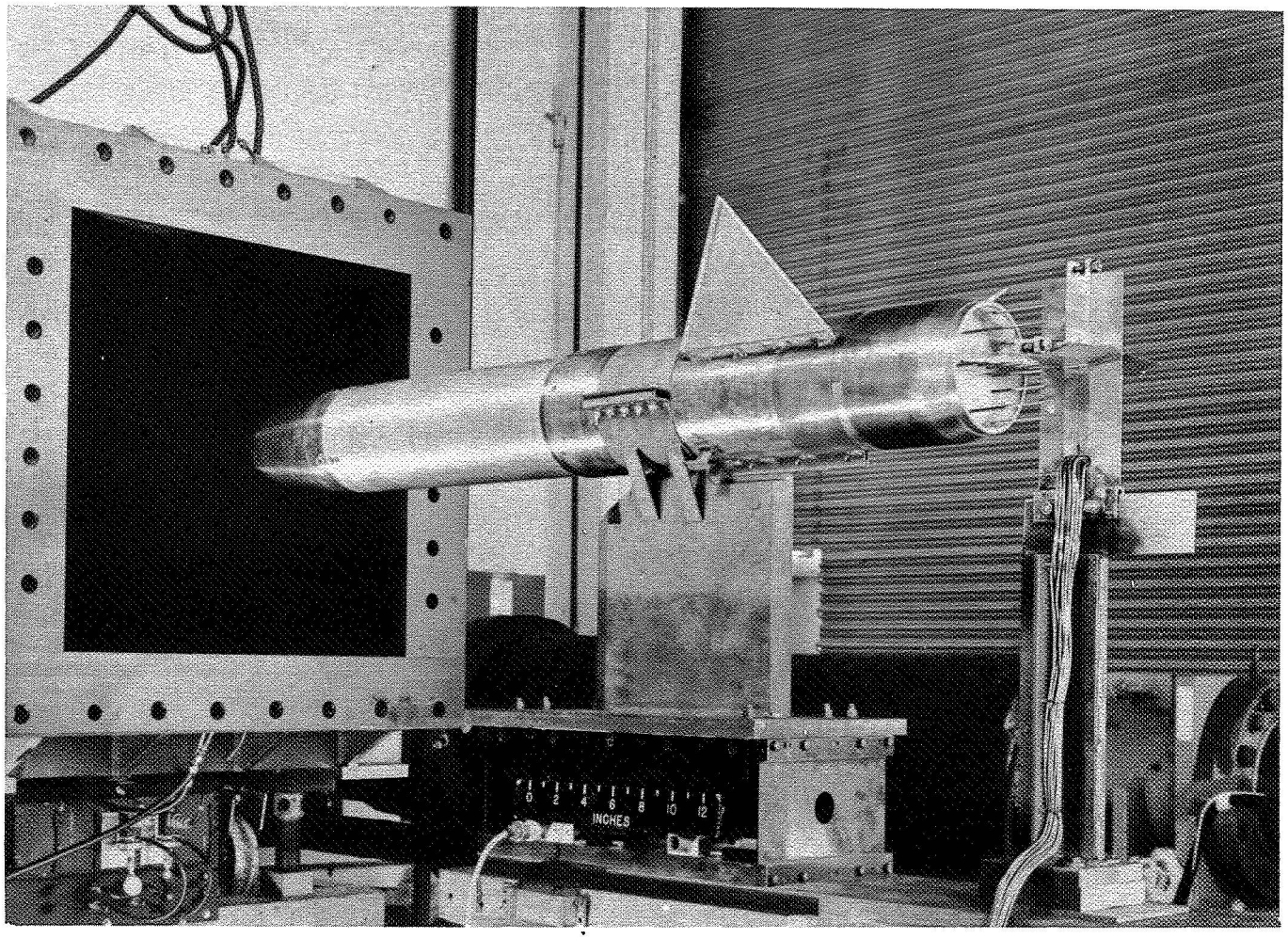

L-58-1092.1

(a) Three-quarter rear view. (Model-exit pressure-survey rake is shown.)

Figure 6.- Model and strut in preflight jet. (Strut supported by thrust stand.)

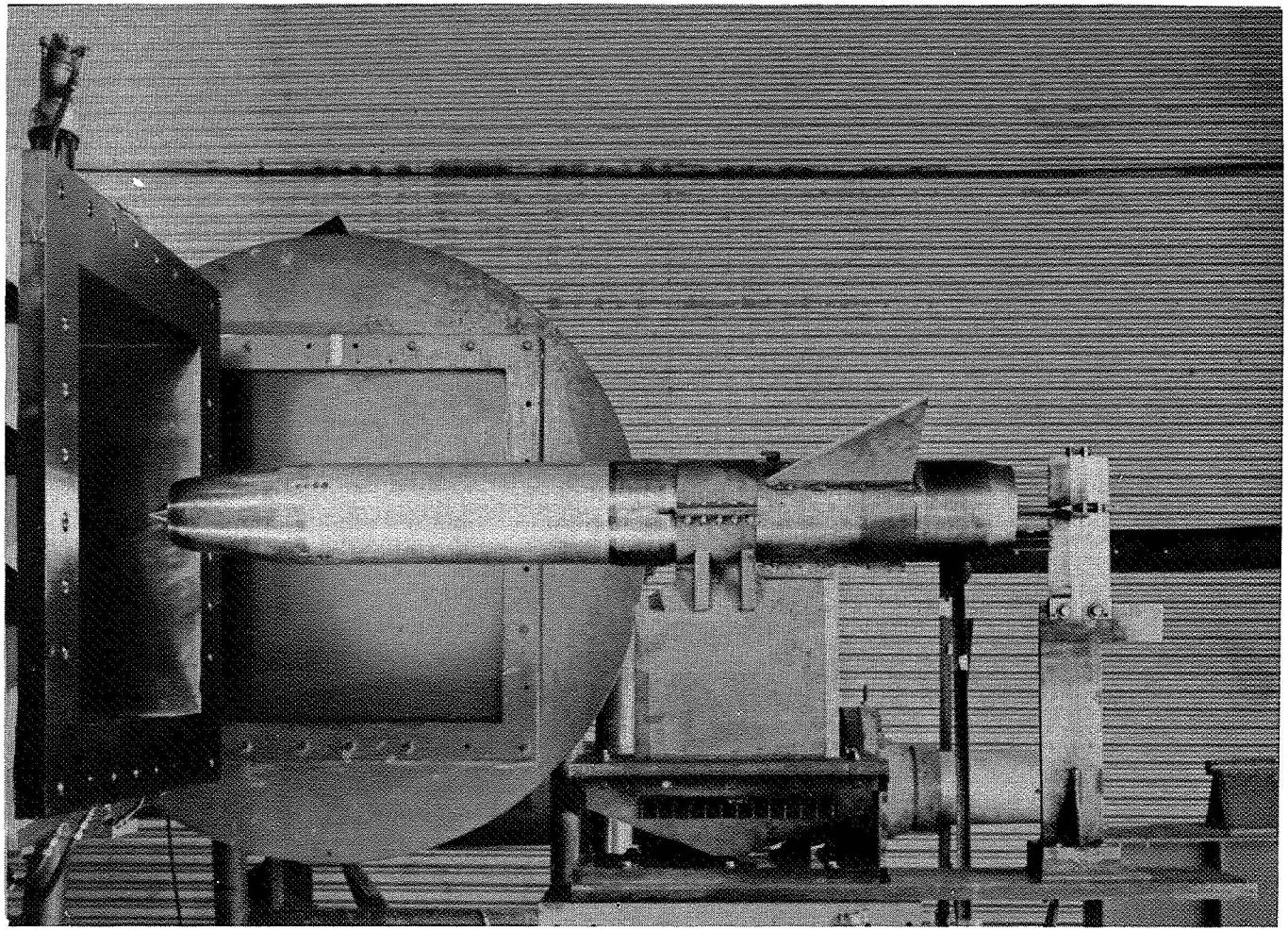

(b) Side view. L-58-1091

Figure 6.- Concluded.

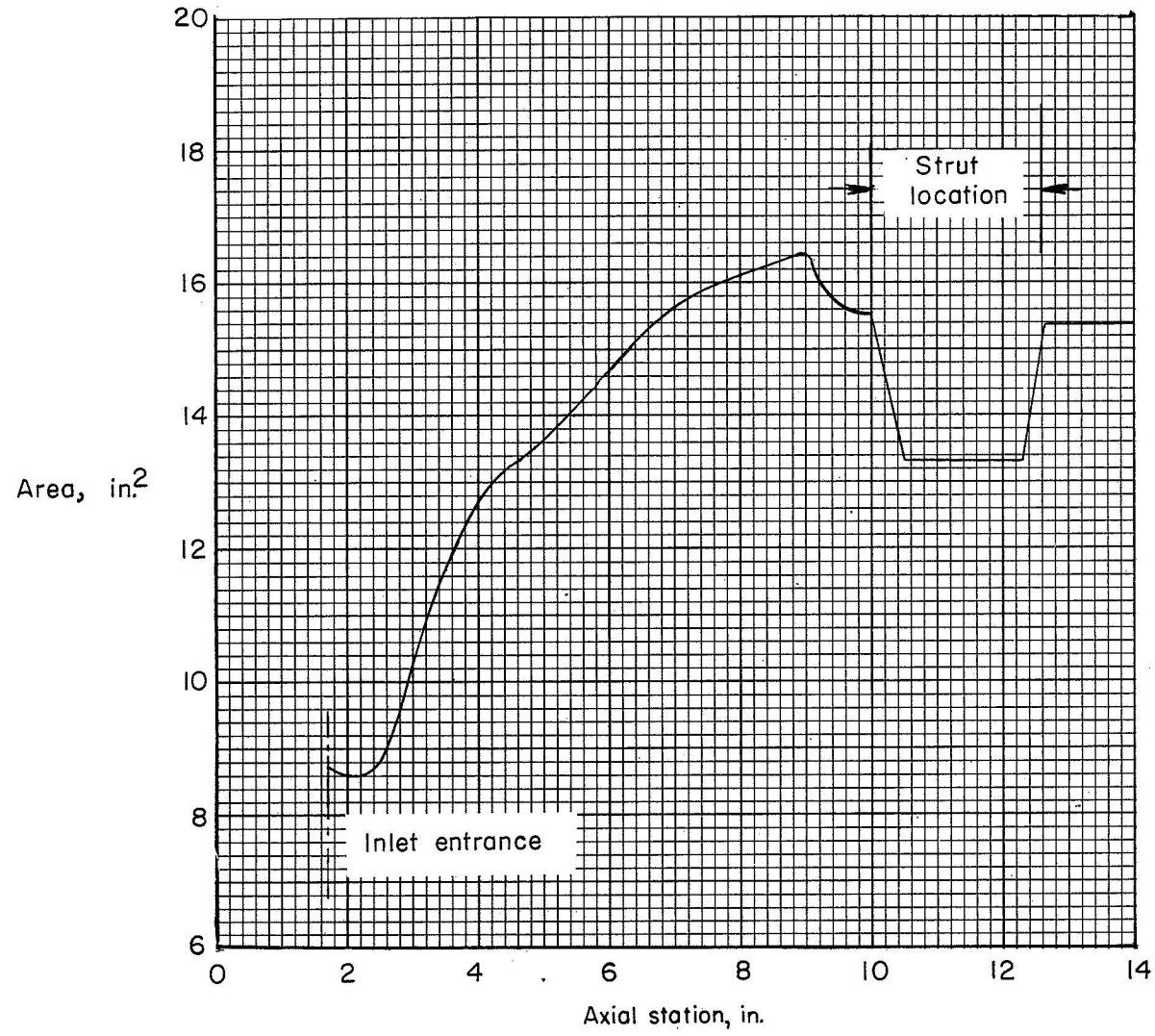

Figure 7.- Diffuser internal-area distribution (fig. 6 of ref. 1). Areas are assumed normal to longitudinal axis.

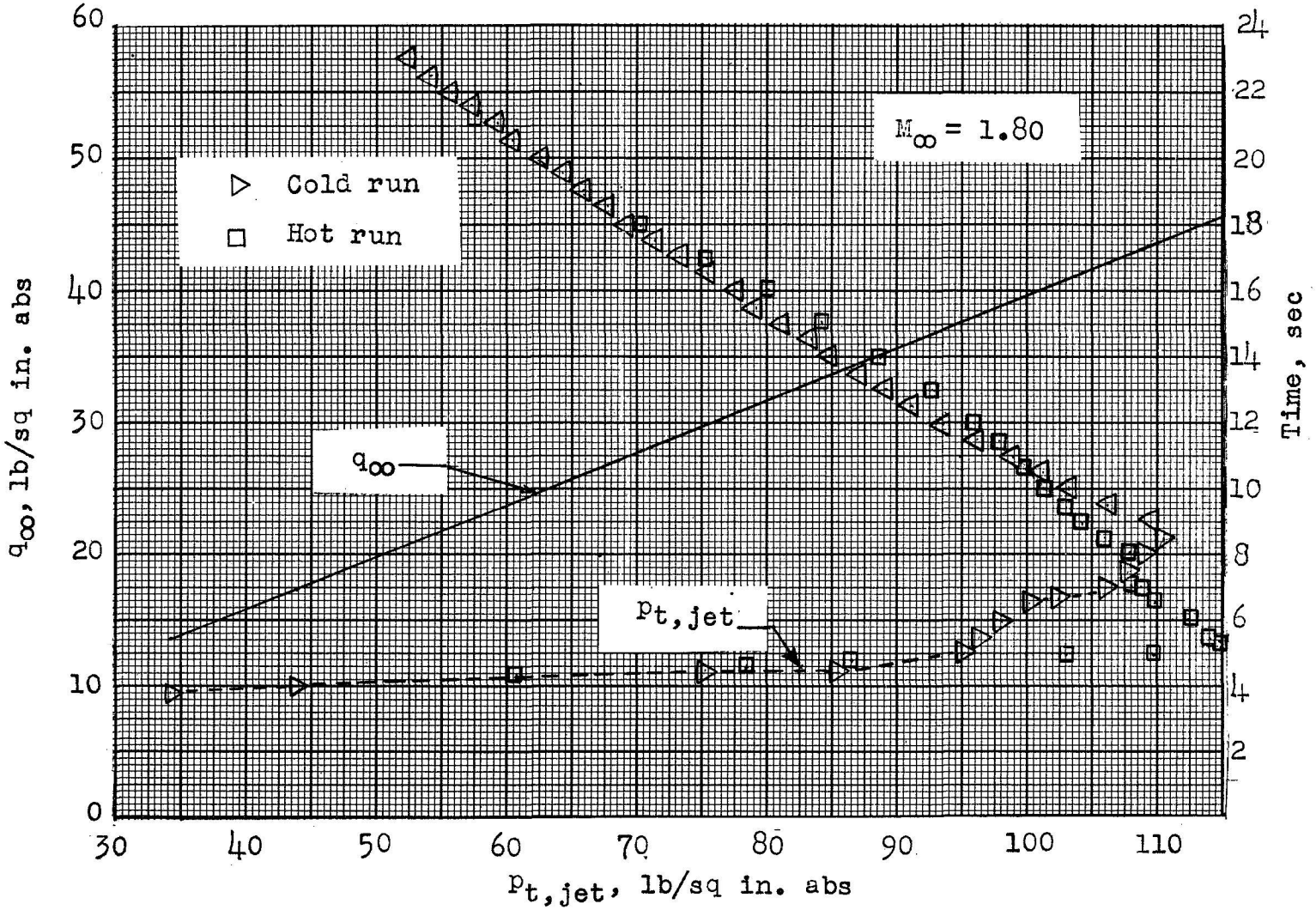

Figure 8.- Variation of free-stream dynamic pressure with jet total pressure and variation of jet total pressure with time. M_∞ = 1.80.

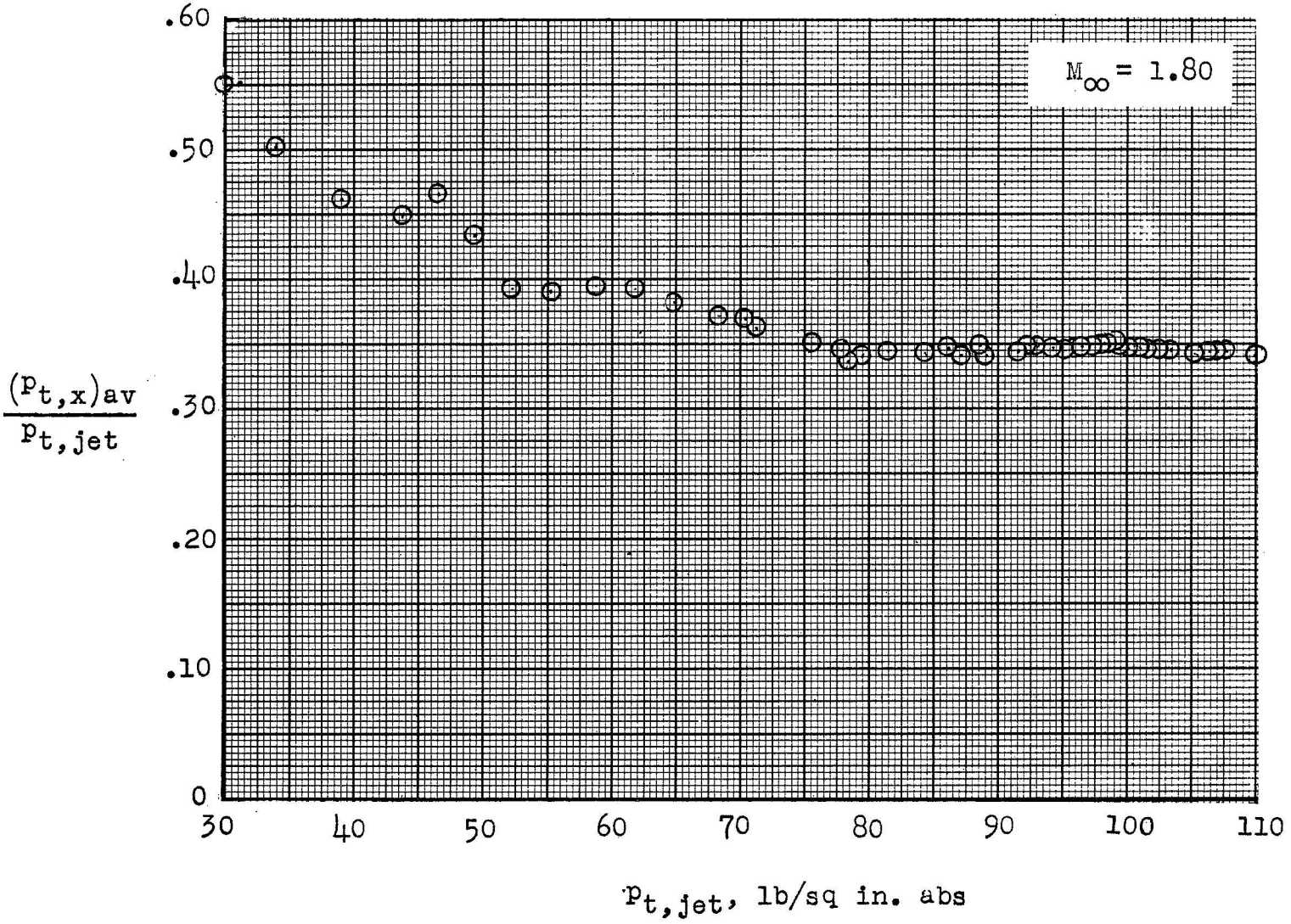

Figure 9.- Combustion-chamber total pressure plotted against free-stream total pressure for cold tests. $M_\infty = 1.80$.

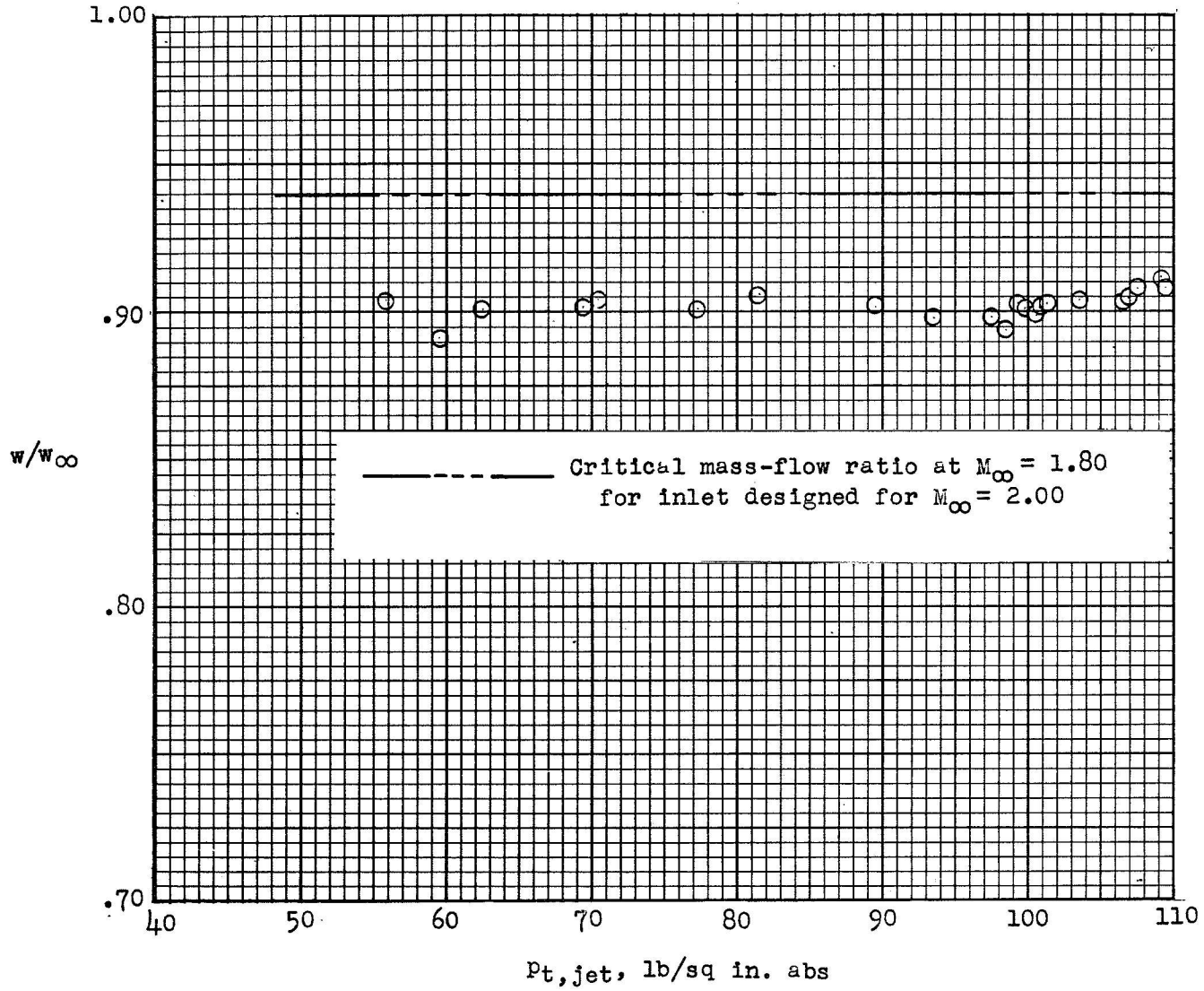

Figure 10.- Inlet mass-flow ratio at a free-stream Mach number of 1.80.

DECLASSIFIED

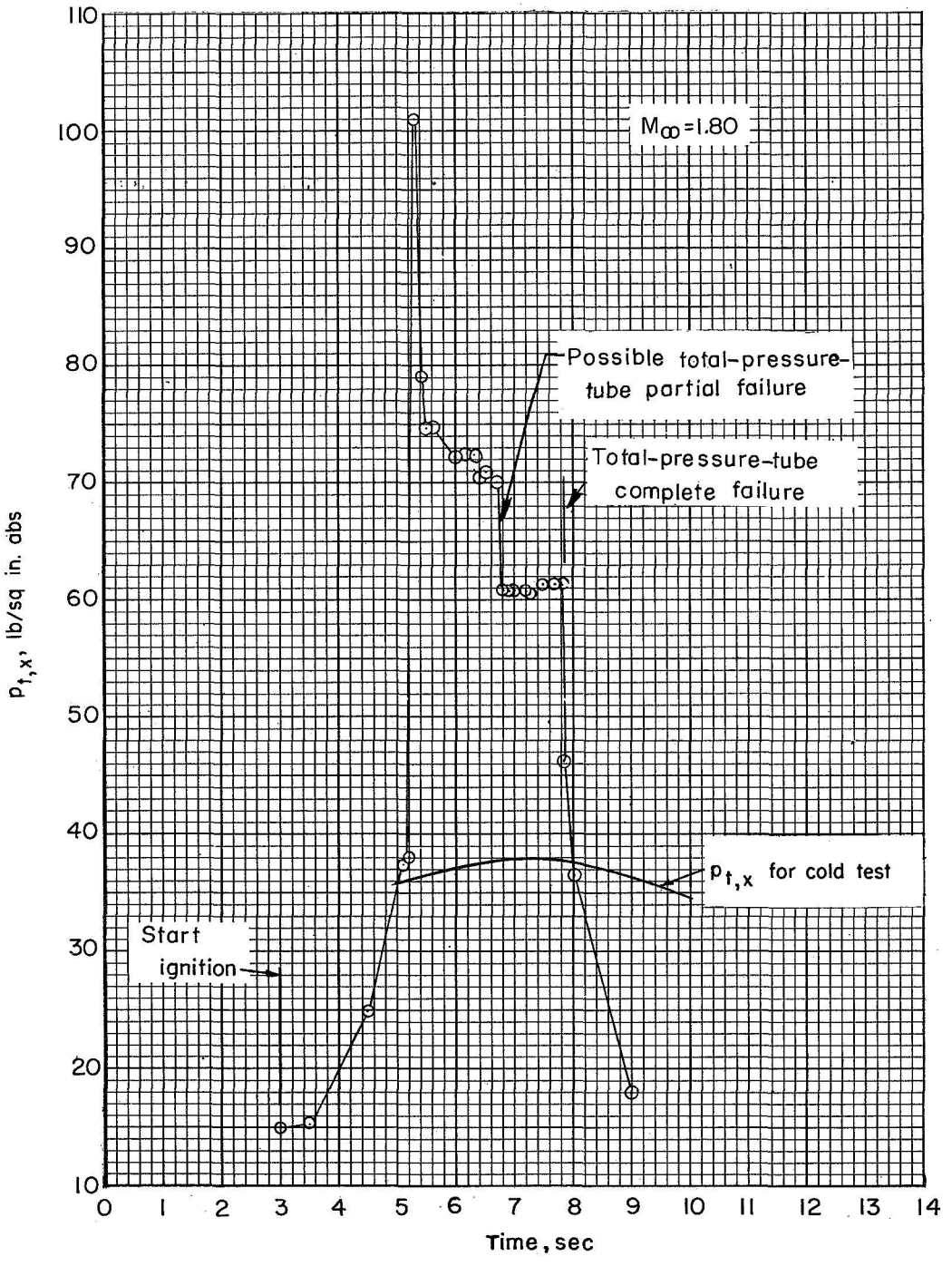

Figure 11.- Variation of total pressure at model exit plane with jet operation time for hot run. Total-pressure tube burned out some time after ignition of sustainer rocket.

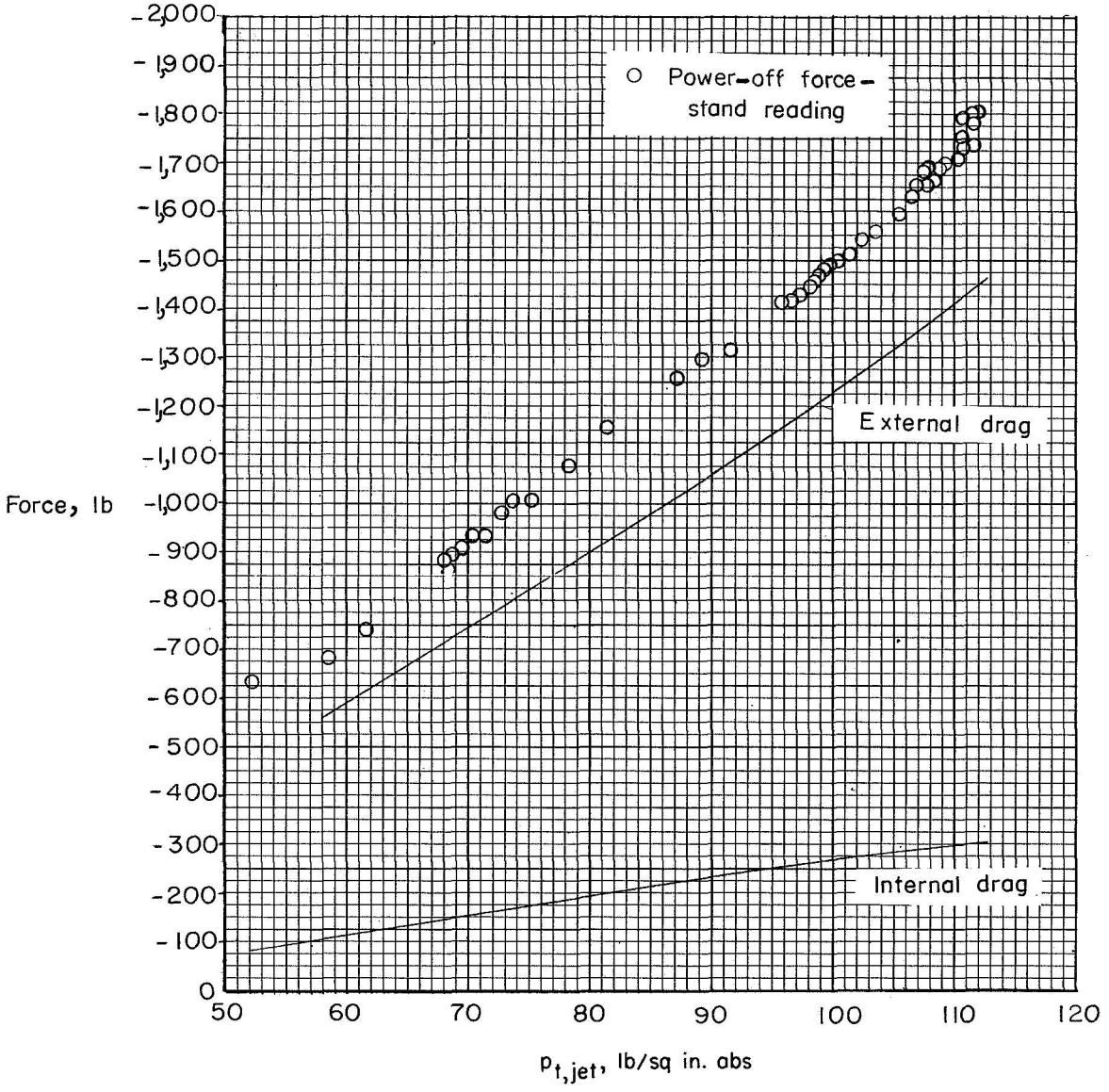

Figure 12.- Power-off ground-test drag measurements (includes strut drag). $M_\infty = 1.80$.

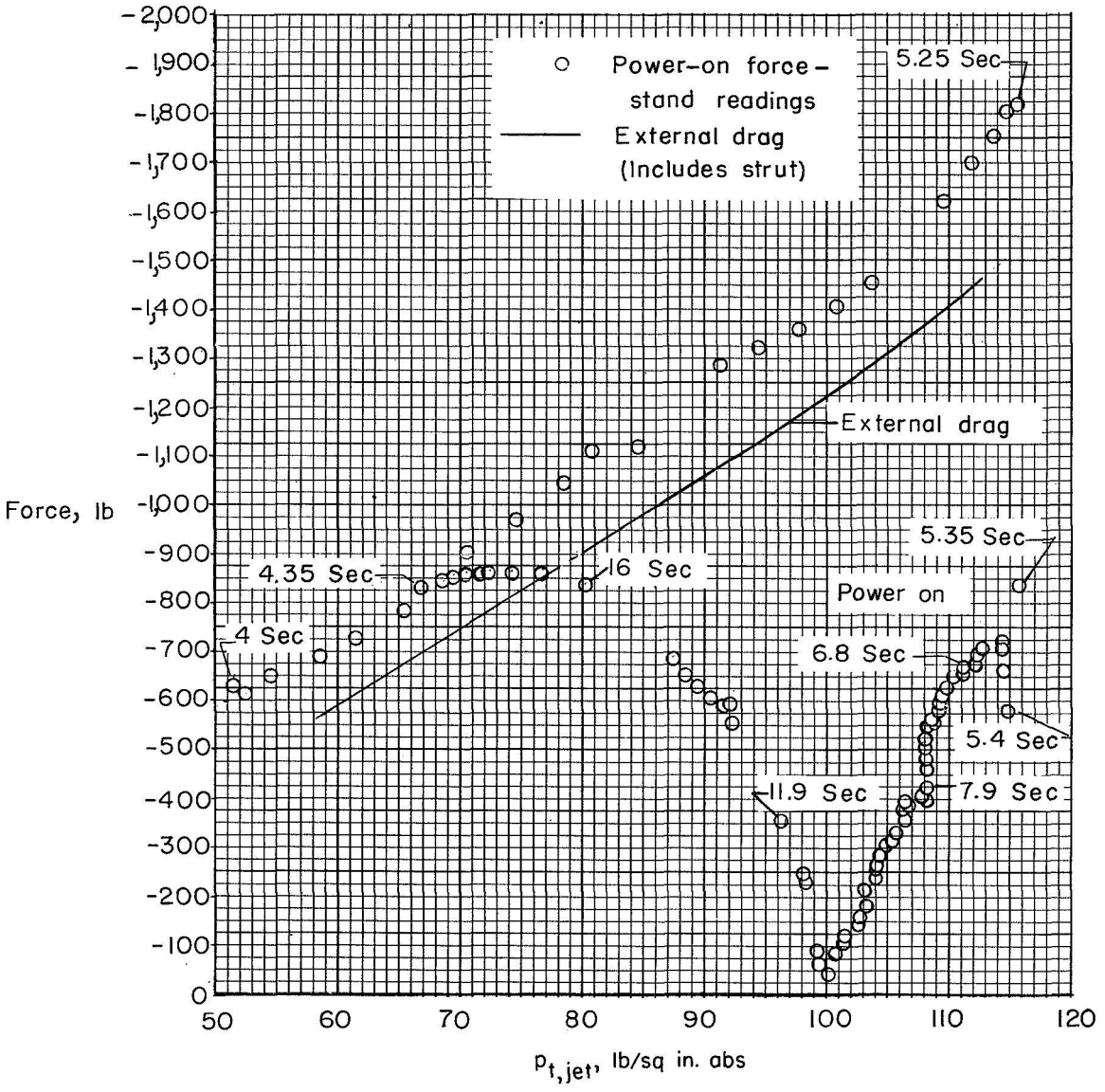

Figure 13.- Power-on ground-test force-stand reading plotted against total pressure of jet. $M_\infty = 1.80$.

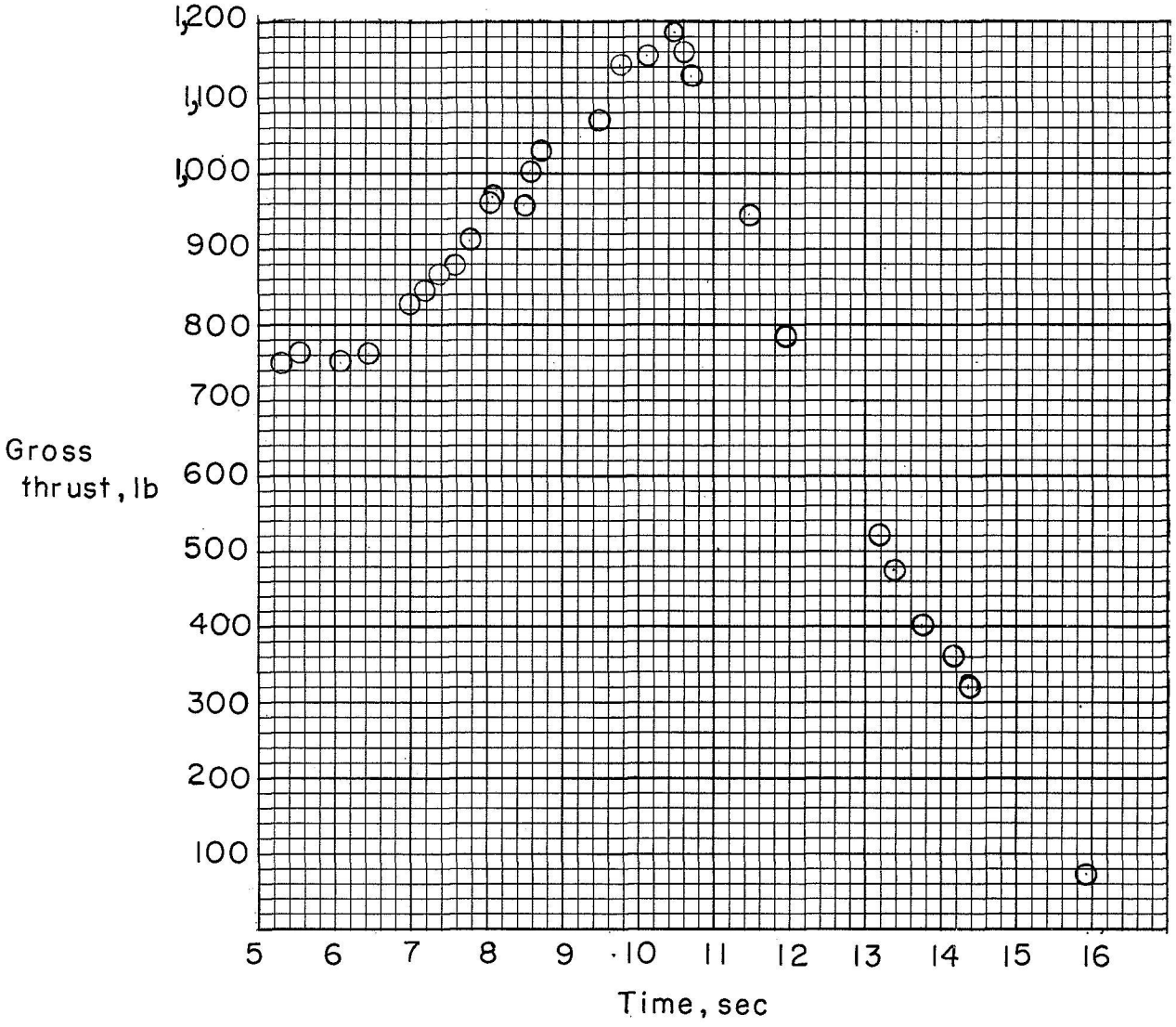

Figure 14.- Ground-test model gross thrust.

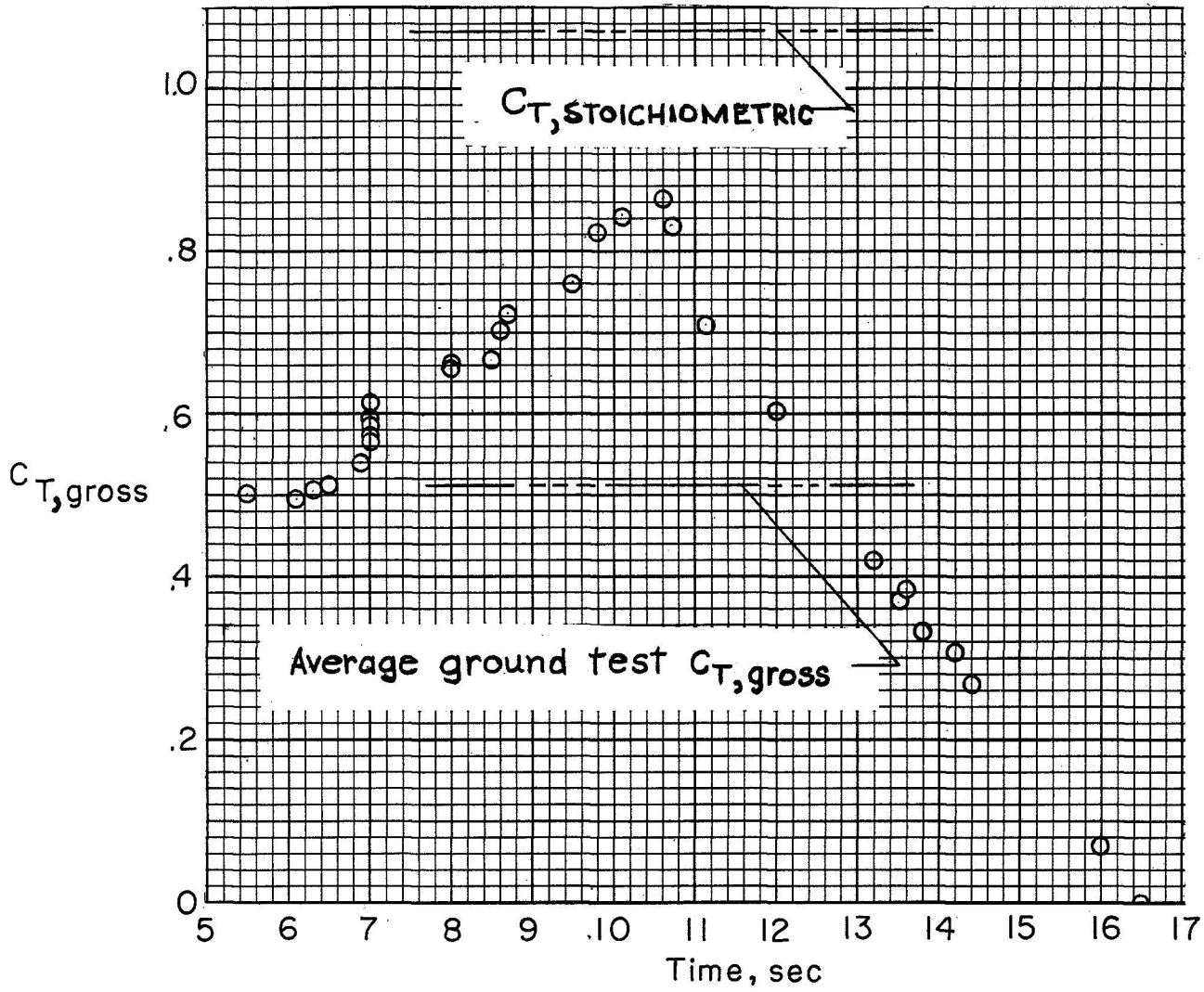

Figure 15.- Gross thrust coefficient for ground tests at a free-stream Mach number of 1.80.

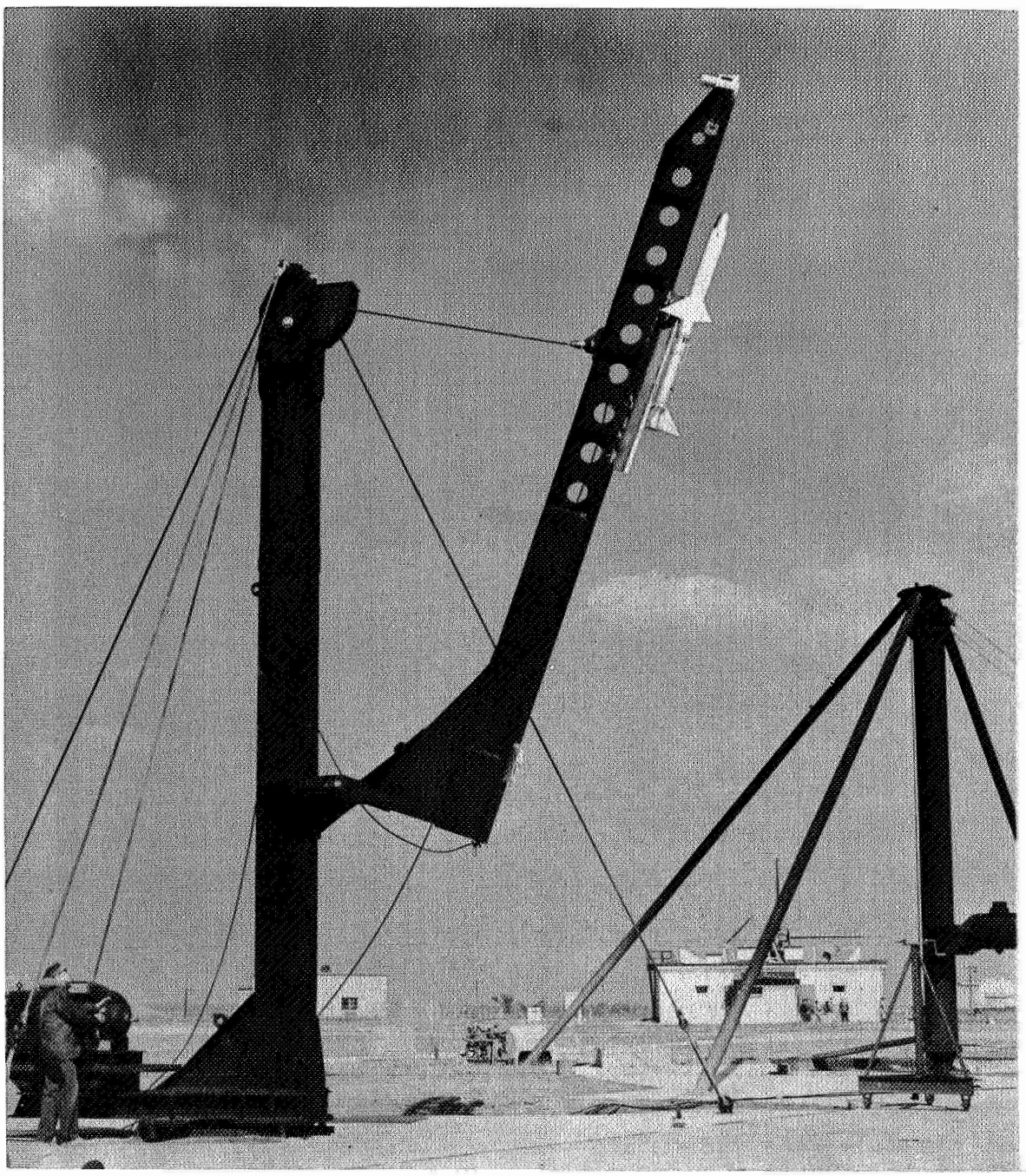

L-58-1205.1

Figure 16.- Model and booster on launcher prior to firing.

DECLASSIFIED

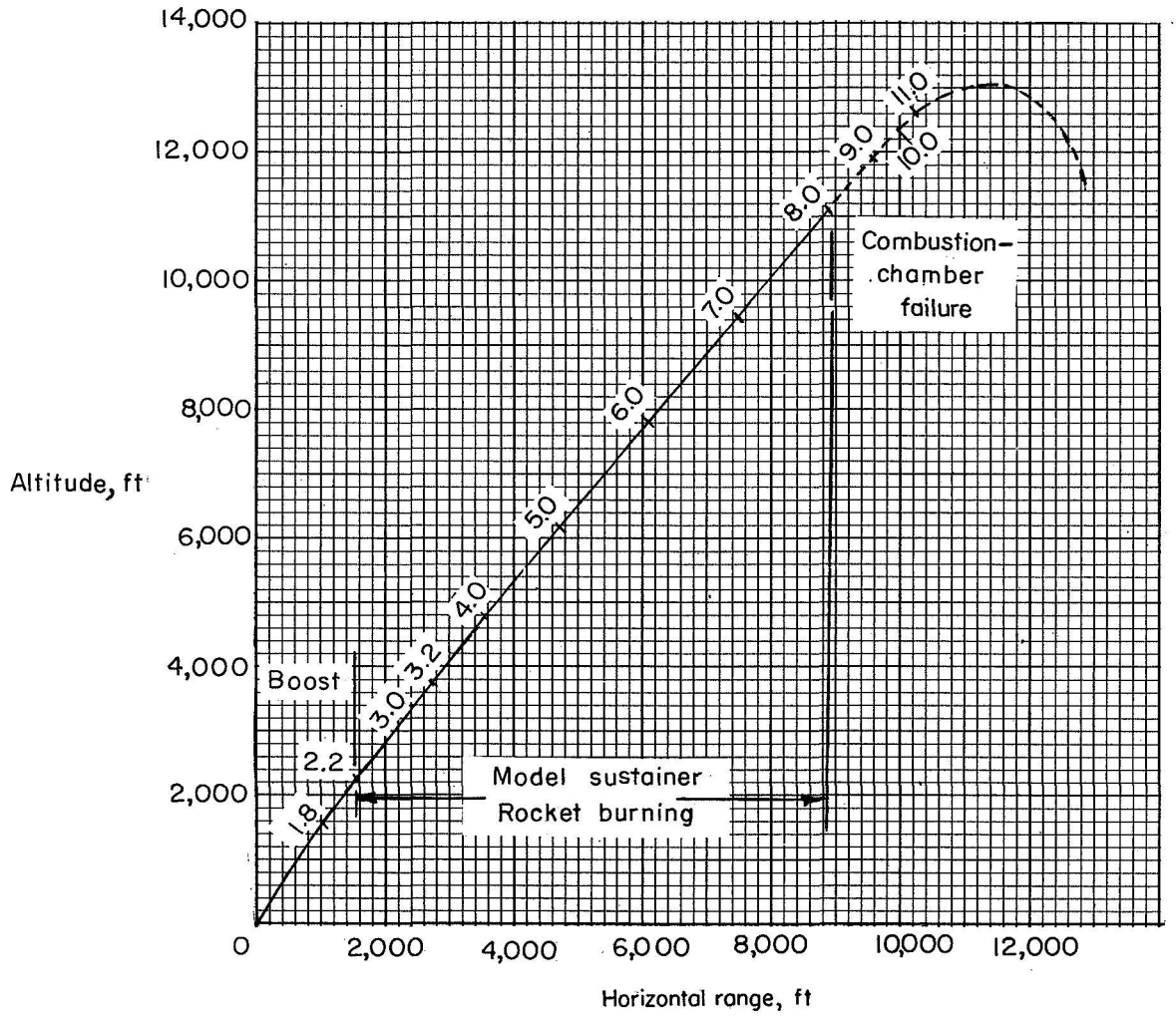

Figure 17.- Altitude plotted against horizontal range for model flight test.

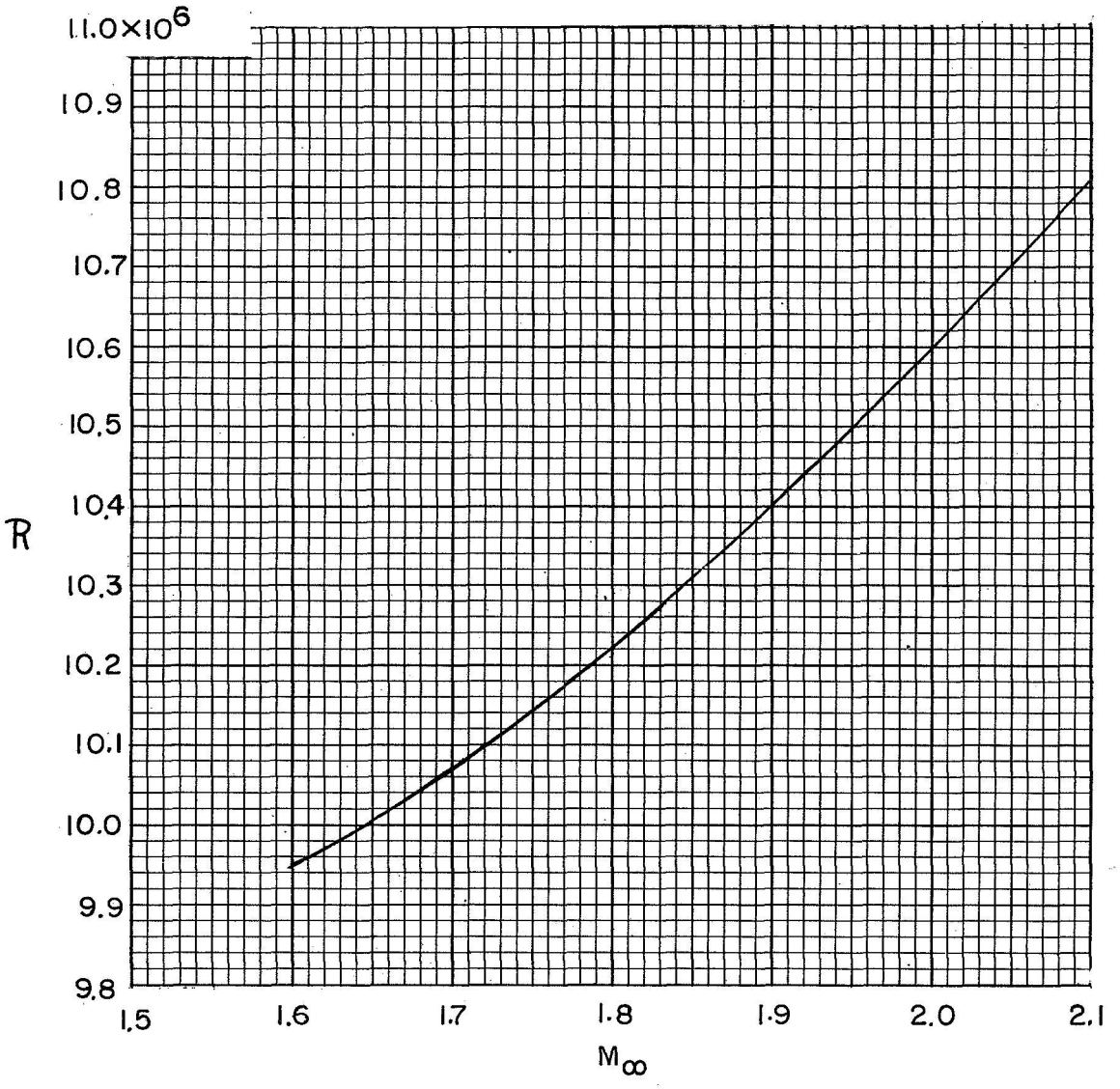

Figure 18.- Variation of Reynolds number per foot with free-stream Mach number over flight Mach number range.

DECLASSIFIED

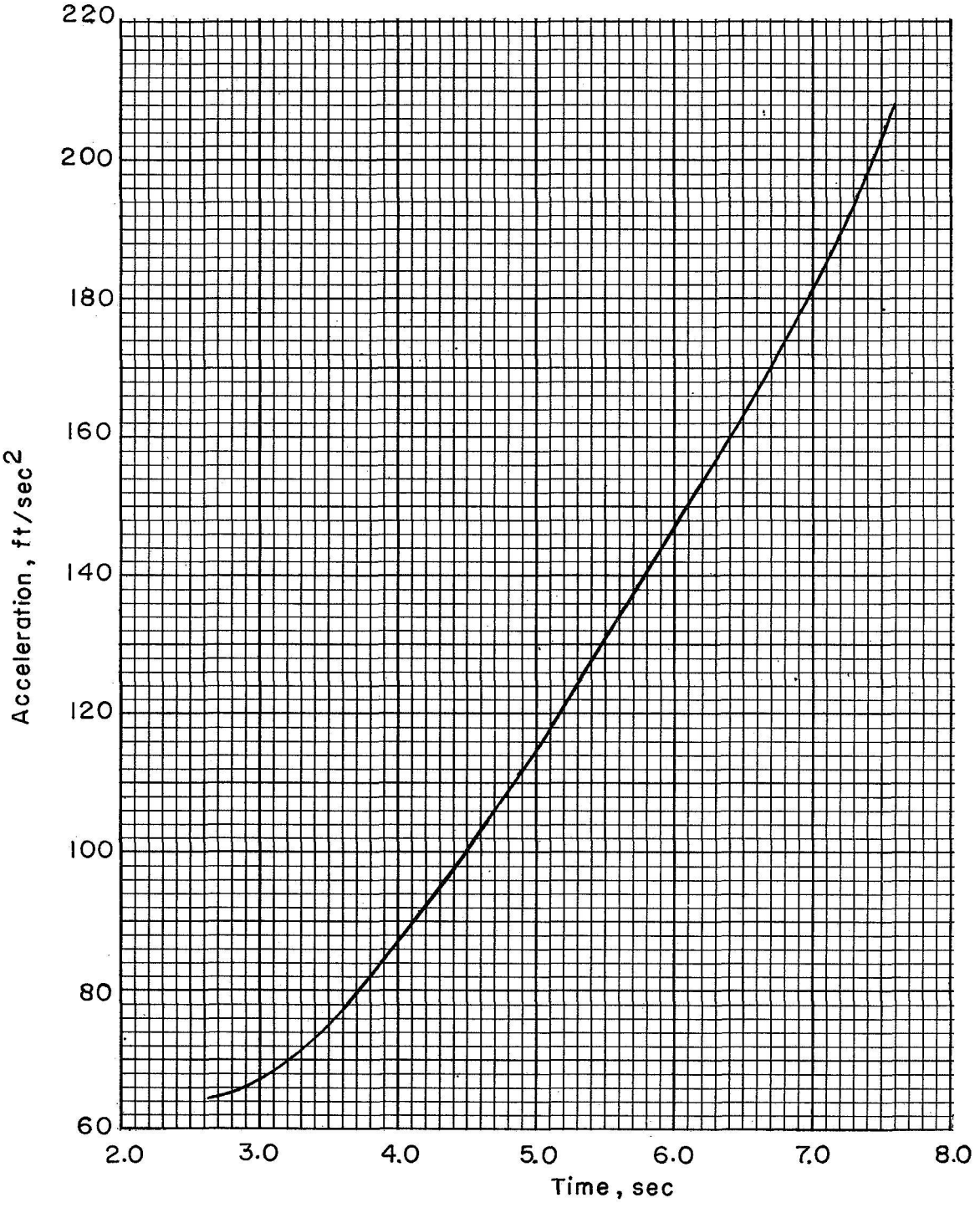

Figure 19.- Acceleration plotted against time for free-flight test.

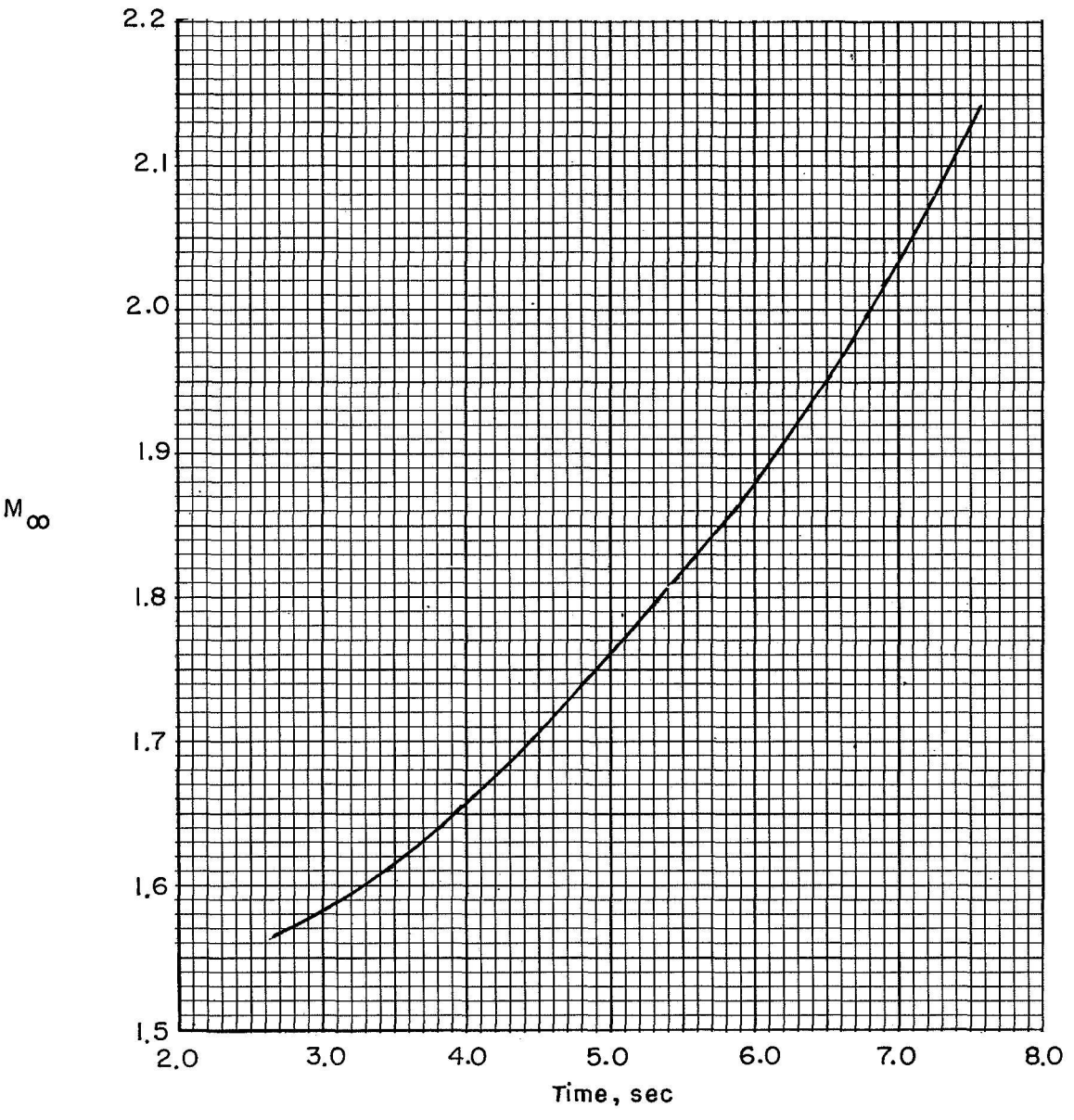

Figure 20.- Mach number plotted against time for flight test.

DECLASSIFIED

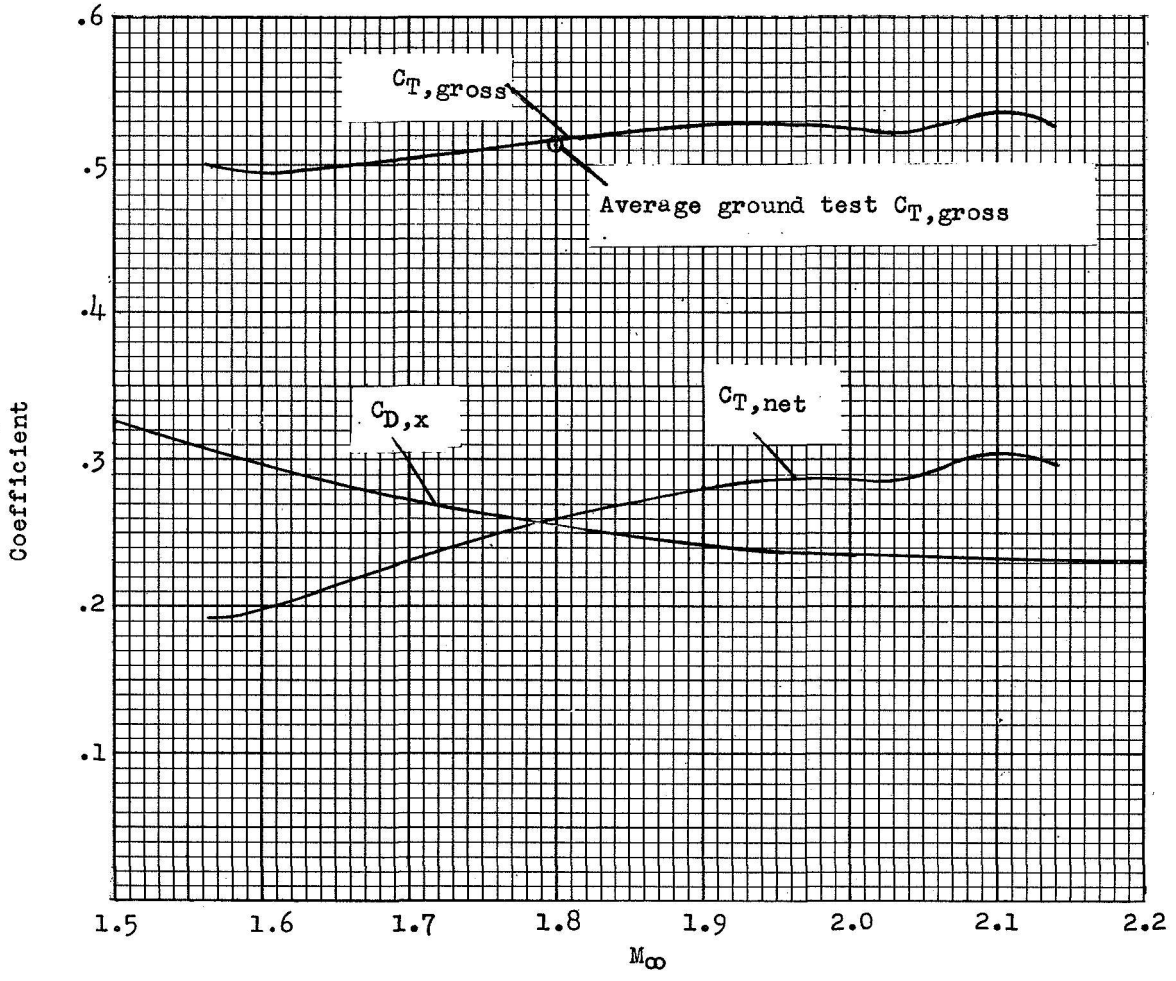

Figure 21.- Plot of net thrust coefficient $C_{T,net}$ from flight data, computed drag coefficient $C_{D,x}$, and resulting gross thrust coefficient $C_{T,gross}$.

$$C_{T,gross} \equiv C_{T,net} + C_{D,x}$$

NOTES: (1) Reynolds number is based on the diameter of a circle with the same area as that of the capture area of the inlet.

(2) The symbol * denotes the occurrence of buzz.

Report and facility	Description			Test parameters				Test data				Performance		Remarks
	Configuration	Number of oblique shocks	Type of boundary-layer control	Free-stream Mach number	Reynolds number $\times 10^{-6}$	Angle of attack, deg	Angle of yaw, deg	Drag	Inlet-flow profile	Discharge-flow profile	Flow picture	Maximum total-pressure recovery	Mass-flow ratio	
CONFID. NASA TM X-29 PARD		1	None	1.56 to 2.14	3.28 to 3.60	0	0	✓				0.90	0.50 to 0.94	
CONFID. NASA TM X-29 PARD	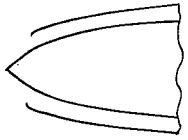	1	None	1.56 to 2.14	3.28 to 3.60	0	0	✓				0.90	0.50 to 0.94	
CONFID. NASA TM X-29 PARD	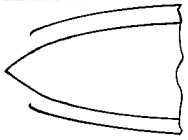	1	None	1.56 to 2.14	3.28 to 3.60	0	0	✓				0.90	0.50 to 0.94	
CONFID. NASA TM X-29 PARD	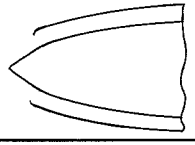	1	None	1.56 to 2.14	3.28 to 3.60	0	0	✓				0.90	0.50 to 0.94	

Bibliography
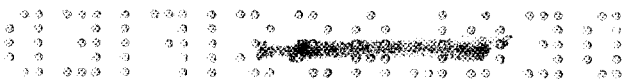
These strips are provided for the convenience of the reader and can be removed from this report to compile a bibliography of NASA inlet reports. This page is being added only to inlet reports.